

Real-Time Kalman Filtering for Nonuniformity Correction on Infrared Image Sequences: Performance and Analysis*

Sergio K. Sobarzo and Sergio N. Torres

Department of Electrical Engineering, University of Concepción,
Casilla 160-C, Concepción, Chile
{ssobarzo, sertorre}@udec.cl
<http://nuc.die.udec.cl>

Abstract. A scene-based method for nonuniformity correction of infrared image sequences is developed and tested. The method uses the information embedded in the scene and performs the correction in a frame by frame Kalman Filter approach. The key assumption of the method is that the uncertainty on the input infrared irradiance integrated by each detector is solved using the spatial infrared information collected from the scene. The performance of the method is tested using infrared image sequences captured by two infrared cameras.

Keywords: Infrared Sensor-Imaging, Infrared Focal Plane Arrays, Signal Processing, Kalman Filtering, Image Coding, Processing and Analysis.

1 Introduction

Infrared (IR) imaging systems are widely used in a variety of civilian and military applications such as aerial surveillance, satellite imaging, early fire detection, biology, robotics, and astronomy [1]. An IR Focal-Plane Array (FPA), the heart of an IR imaging system, is an array consisting in a mosaic of photo-detector elements that are placed in the focal plane of the optical imaging system [3].

It is well known that the performance of the whole IR imaging system is strongly affected by the fixed-pattern noise (FPN) [1]. The FPN, also called nonuniformity, is the unequal photoresponse of the detectors in the FPA when an uniform scene is imaged. What makes the FPN even a more challenging problem is that the spatial nonuniformity slowly drifts in time, and depending on the technology used, the drift can take from minutes to hours [1]. The task of any nonuniformity correction (NUC) technique is to compensate for the spatial nonuniformity and updates the compensation as needed to account for the temporal drift in the detector's response [2], [5], [6].

* This work was partially supported by Grant Milenio ICM P02-049. S. Sobarzo acknowledges support from Conicyt. The authors wish to thank Ernest E. Armstrong (OptiMetrics Inc., USA) and Pierre Potet (CEDIP Infrared Systems, France) for collecting the data.

In this paper, a new algorithm for NUC in IR-FPA, based on Kalman filter (KF) theory, is developed and tested. The algorithm operates, per pixel and in a frame by frame basis, assuming that the nonuniformity parameters, the gain and bias, follow a Gauss-Markov model (GMM). As the method operates, the autocorrelation parameters of the gain and bias are fixed to be close enough to one, following GMM's convergence requirements. The per pixel input irradiance parameter is computed on-line using a spatial lowpass filter [4]. The performance of the algorithm is tested using sequences of corrupted IR data captured by two infrared cameras and is compared against the results obtained by using black body radiator corrected data. Further, the algorithm is also tested over a image sequence with artificial nonuniformity. Two performance parameters are computed to check the level of reduction of the nonuniformity.

2 Algorithm

2.1 Mathematical Modelling

The model for each pixel of the IR-FPA is a linear relationship between the input irradiance and the detector response [1,7]. Further, for a single detector in the FPA, the linear input-output relation of the ij -th detector in the k -th frame is approximated by [1]:

$$Y_k^{ij} = A_k^{ij} T_k^{ij} + B_k^{ij} + V_k^{ij} \quad (1)$$

where A_k^{ij} and B_k^{ij} are the ij -th detector's gain and bias, respectively, at the k -th frame. T_k^{ij} represents the average number of photons that are detected by the ij -th detector during the integration time associated with the k -th frame. V_k^{ij} is the additive readout (temporal) noise associated to the ij -th detector for the k -th frame. For simplicity of notation, the pixel superscripts ij will be omitted with the understanding that all operations are performed on a pixel-by-pixel basis.

In this paper, nonuniformity's slow drift between frames is modeled by a Gauss-Markov process for the gain and the bias of each pixel on the FPA. This is:

$$\mathbf{X}_k = \Phi_{k-1} \mathbf{X}_{k-1} + \mathbf{G}_{k-1} \mathbf{W}_{k-1} \quad (2)$$

where \mathbf{X}_k is the state vector comprising the gain A_k and the bias B_k at the k -th frame and Φ_k is the 2×2 transition diagonal matrix between the states at k and $k - 1$, with its diagonal elements being the parameters α_k and β_k that represent, respectively, the level of drift in the gain and bias between consecutive frames. \mathbf{G}_k is a 2×2 noise identity matrix that randomly relates the driving (or process) noise vector \mathbf{W}_k to the state vector \mathbf{X}_k . The components of \mathbf{W}_k are $W_k^{(1)}$ and $W_k^{(2)}$, the random driving noise for the gain and the bias, respectively, at the k -th frame. A key practical requirement to be set on the model is that, between frames, the drift in the gain and bias is very low; therefore, the drift

parameters α_k and β_k have to be set to values closer but not equal to one. All others assumptions are shown and justified in detail elsewhere [7].

Also, in this paper the observation model for a given frame can be cast as:

$$\mathbf{Y}_k = \mathbf{H}_k \mathbf{X}_k + \mathbf{V}_k \tag{3}$$

where \mathbf{H}_k is the observation vector in which the first element contains the input T_k per frame and \mathbf{V}_k is the additive temporal noise. The main assumption in (3) is that the input T_k in any detector is a known parameter. Further, T_k is estimated, for each pixel, using a lowpass spatial filter that can emulate the IR radiation and it lessens the effect of the gain and bias difference between neighboring pixels. The mask size (number of neighboring pixels) must be determined according to the type of the scene imaged and to the amount of nonuniformity.

The \mathbf{T}_k value is estimated averaging the pixel neighborhood. We can assume that a pixel and their near neighbor is illuminating by the same infrared radiance. Averaging the neighboring of a pixel i,j and assuming $\mathbf{A}_{i,j} = 1, \mathbf{B}_{i,j} = 0, \mathbf{V}_{i,j} = 0$ and $T_{i,j} = T$ inside the neighborhood we have:

$$\bar{Y}_k^{ij} = \bar{A}_k^{ij} \bar{T}_k^{ij} + \bar{B}_k^{ij} + \bar{V}_k^{ij} = T_k^{ij} \tag{4}$$

2.2 Kalman Filter Equations

The main idea is to develop an algorithm, based on the KF theory [9], that estimates frame by frame the gain and bias of each pixel using each incoming frame from the read-out data.

The recursive equations of the KF to estimate the parameters (the \mathbf{X}_k vector) are the following [8]:

$$\hat{\mathbf{X}}_k = (\Phi_{k-1} - \mathbf{K}_k \mathbf{H}_k) \hat{\mathbf{X}}_{k-1} + \mathbf{K}_k \mathbf{Y}_k \tag{5}$$

where $\hat{\mathbf{X}}_{k+1}$ and $\hat{\mathbf{X}}_k$ are the estimated gain and bias at the k -th and $k - 1$ -th frame, respectively. \mathbf{K}_k is the Kalman gain vector defined by:

$$\mathbf{K}_k = \Phi_{k-1} \mathbf{P}_{k-1} \mathbf{H}'_k \mathbf{F}_k^{-1} \tag{6}$$

where $\mathbf{R}_{k-1} = Var(\mathbf{V}_{k-1})$ and $\mathbf{F}_k = \mathbf{H}_k \mathbf{P}_{k-1} \mathbf{H}'_k + \mathbf{R}_{k-1}$

The recursive equation to compute the error covariance matrix \mathbf{P}_k is:

$$\mathbf{P}_k = \Phi_{k-1} (\mathbf{P}_{k-1} - \mathbf{P}_{k-1} \mathbf{H}'_k \mathbf{F}_k^{-1} \mathbf{H}_k \mathbf{P}_{k-1}) \Phi'_{k-1} + \mathbf{G}_{k-1} \mathbf{Q}_{k-1} \mathbf{G}'_{k-1} \tag{7}$$

with $\mathbf{Q}_{k-1} = Var(\mathbf{W}_{k-1})$. The first values that must to feed the recursive equations (5,6,7) are: $\hat{\mathbf{X}}_0 = E(\mathbf{X})$ and $\mathbf{P}_0 = Var(\mathbf{X})$, which must be known.

3 Performance Analysis

The main goal of this section is to test the ability of the proposed NUC method to mitigate nonuniformity as well as to follow the drift in the nonuniformity

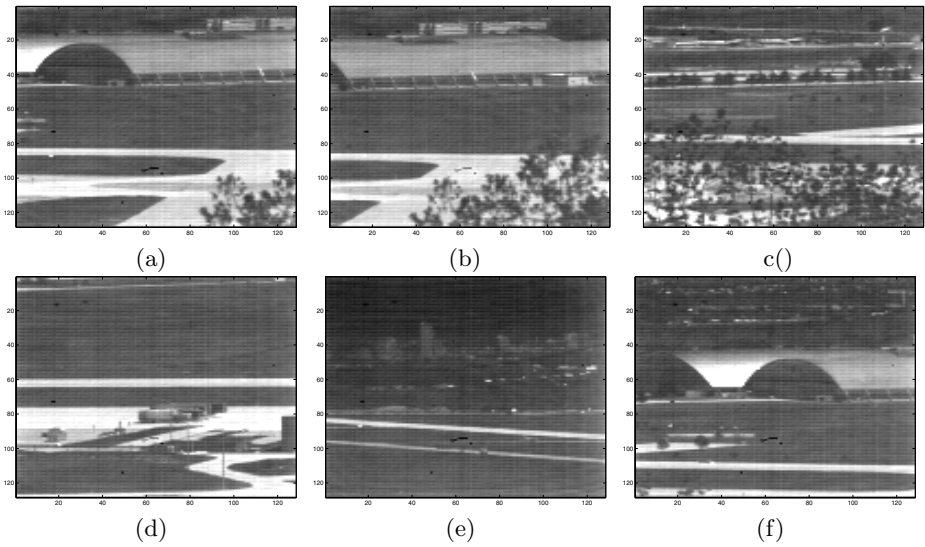


Fig. 1. Six frames of an IR sequence with real NonUniformity. a) The 10 – *th* frame. b) The 100 – *th* frame. c) The 1000 – *th* frame. d) The 2000 – *th* frame. e) The 3000 – *th* frame. f) The 4000 – *th* frame.

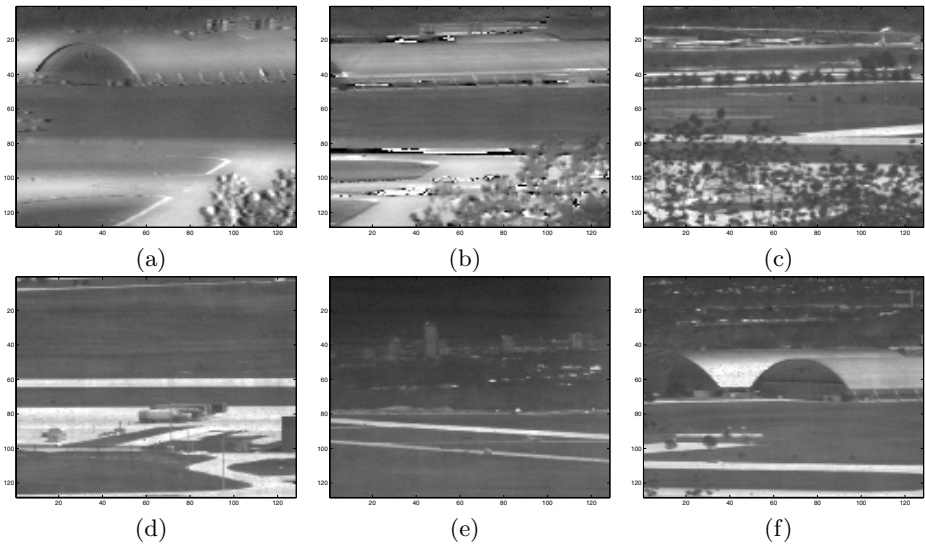


Fig. 2. The six frames of the IR sequence shown in figure 1 corrected using the proposed algorithm. a) The 10 – *th* frame. b) The 100 – *th* frame. c) The 1000 – *th* frame. d) The 2000 – *th* frame. e) The 3000 – *th* frame. f) The 4000 – *th* frame.

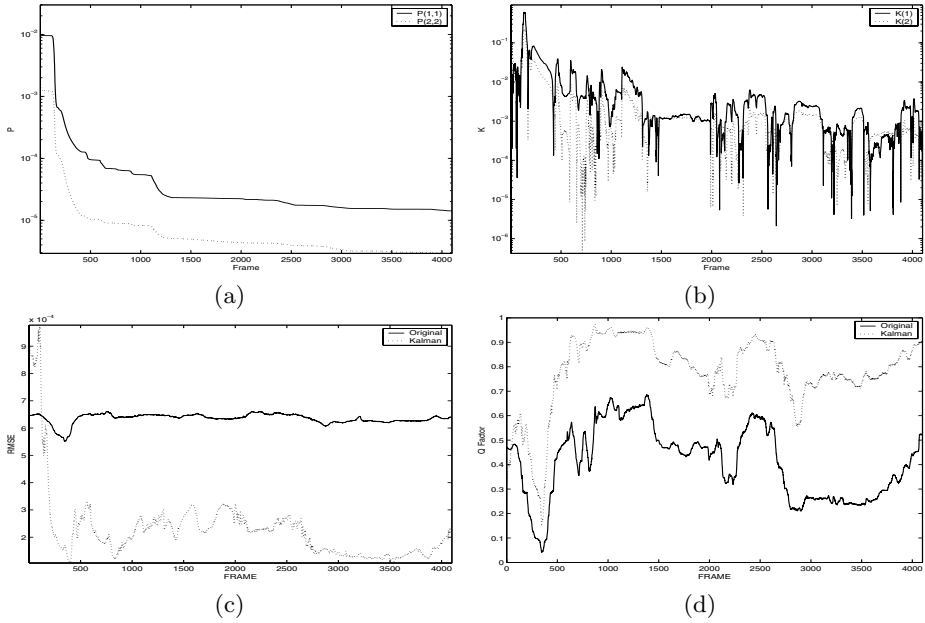


Fig. 3. a) Diagonal elements of the error covariance matrix \mathbf{P}_k versus frame time for the algorithm applied to figure 1 sequence. b) Kalman gain matrix \mathbf{K}_k versus frame time. c) RMSE between the real noisy data and the corrected data with the data corrected with a Black Body technique (true data). d) Q Factor between the real noisy data and the corrected data with the data corrected with a Black Body technique (true data).

parameters. The algorithm is tested with real infrared image sequences capture by two cameras. The first sequence has been collected using a 128×128 InSb FPA cooled camera (Amber Model AE-4128) operating in the $3 - 5\mu\text{m}$ range. The collected data is quantized with 16 bits @ 30fps. The figure 1 shows raw frames of the sequence and figure 2 shows the corresponding frames corrected with the proposed algorithm. As expected, it can be seen using the naked eye that the method reach a good nonuniformity correction in the $1000 - \text{th}$ frame and after.

The evolution of the error covariance matrix \mathbf{P}_k along the frame time is showed in the figure 3 (a), while the evolution of the Kalman gain matrix along the frame time is shown in the figure 3 (b). As expected, it can be seen a reduction in the diagonal elements of the covariance matrix as long as the method is processing the incoming infrared information, converging therefore to the estimation of the real nonuniformity parameters.

As a numerical measure of the performance of the proposed algorithm, the parameters RMSE [12] and the Q factor [11] are computed between a true image(a one corrected in the laboratory with black bodies radiators) and the real

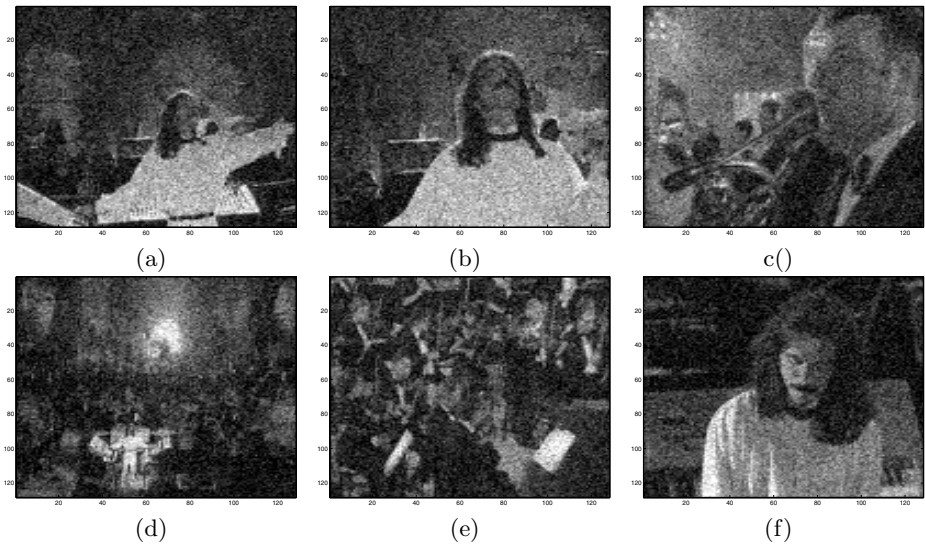


Fig. 4. Six frames of a video sequence with simulated nonuniformity. a) The 10 - *th* frame. b) The 100 - *th* frame. c) The 1000 - *th* frame. d) The 2000 - *th* frame. e) The 3000 - *th* frame. f) The 4000 - *th* frame .

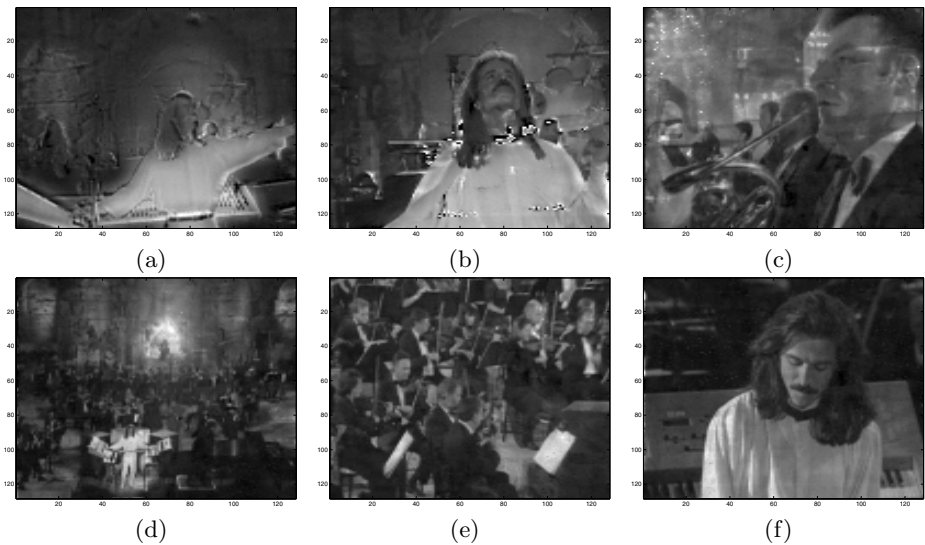


Fig. 5. The frames of figure 4 corrected using the proposed algorithm. a) The 10 - *th* frame. b) The 100 - *th* frame. c) The 1000 - *th* frame. d) The 2000 - *th* frame. e) The 3000 - *th* frame. f) The 4000 - *th* frame.

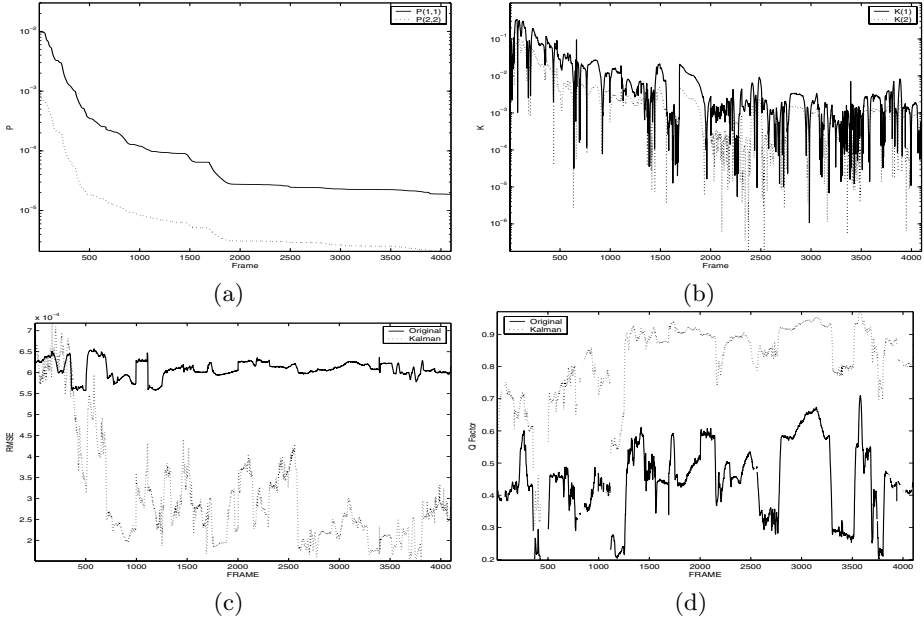


Fig. 6. a) The diagonal elements of the error covariance matrix \mathbf{P}_k versus frame time for the algorithm applied to figure 4 sequence. b) The Kalman gain matrix \mathbf{K}_k versus frame time. c) The RMSE between the the noisy image and the corrected data with the true image. d) Q Factor between the noisy image and the corrected data with the true image.

image (image with FPN) or the image corrected with our method. The RMSE is defined as follow:

$$RMSE = \frac{1}{n} \sqrt{\sum_{i=1}^n (Y_i^t - Y_i^c)^2} \tag{8}$$

where n is the total number of pixels, and Y_i^t is the i -th value on the true image. Y_i^c is the i -th value of the corrected image or the real image.

The recently published Q Factor is a measure of three desirable features between two images (the true and corrected): correlation, luminance distortion and contrast modification. The dynamic range of the Q Factor is $[-1, 1]$. The best value is 1, and it is achieved only if the true image is identical to the compensated image.

$$Q = \frac{\sigma_{Y^t Y^c}}{\sigma_{Y^t} \sigma_{Y^c}} \cdot \frac{2\bar{Y}^t \bar{Y}^c}{(\bar{Y}^t)^2 + (\bar{Y}^c)^2} \cdot \frac{2\sigma_{Y^t} \sigma_{Y^c}}{\sigma_{Y^t}^2 + \sigma_{Y^c}^2} \tag{9}$$

The RMSE and the Q factor between the noisy real sequence and the corrected sequence with the proposed algorithm with a corrected sequence using

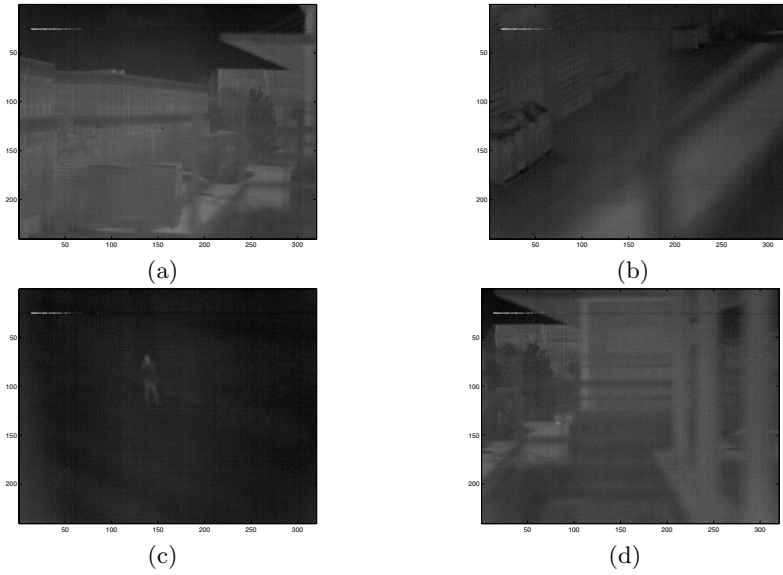


Fig. 7. Four frames with real NonUniformity. a) The 10 - *th* frame. b) The 100 - *th* frame. c) The 1000 - *th* frame. d) The 1500 - *th* frame.

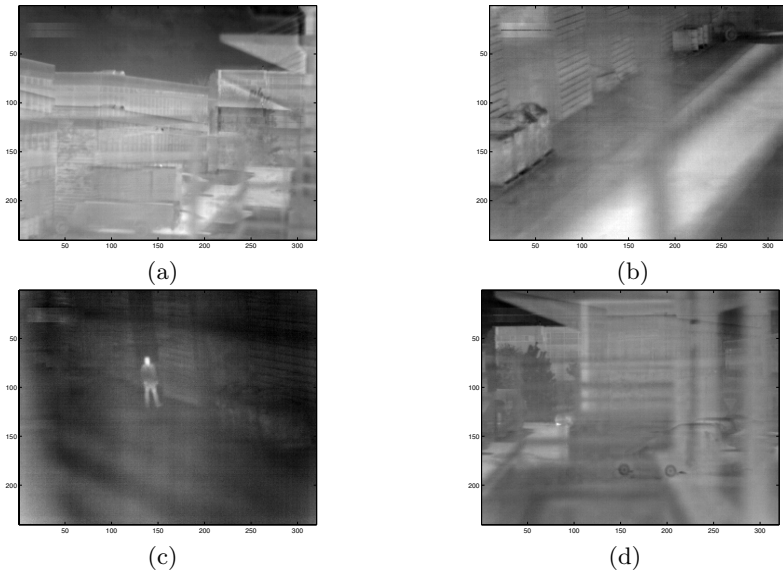


Fig. 8. The four previous frames corrected with the new technique. a) The 10 - *th* frame. b) The 100 - *th* frame. c) The 1000 - *th* frame. d) The 1500 - *th* frame .

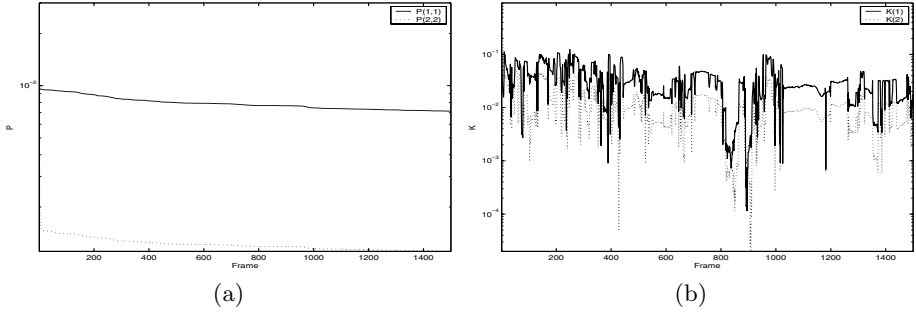


Fig. 9. a) The diagonal elements of the error covariance matrix \mathbf{P}_k versus the frame time for the algorithm applied to figure 7 sequence. b) The Kalman gain matrix versus the frame time \mathbf{K}_k .

a Black Body technique is represented in the figure 3 (c) and the figure 3 (d) respectively. It can be seen a notably numerical reduction in the RMSE after the 500th frame. It can be also seen a notably better performance on the Q factor after the 500th frame.

The developed algorithm is also applied to an infrared video sequence with simulated nonuniformity. The video sequence was created adding artificial noise to 4100 true frames (frames without nonuniformity). As an example, figure 4 shows images with artificial nonuniformity. The corresponding corrected frames are shown in figure 5. The evolution of \mathbf{P}_k , \mathbf{K}_k the RMSE and Q factor is represented in figure 6. The goal of this test is to check the performance of the method with images with a level of nonuniformity more severe than real cases. It can be seen that the method presents a similar performance to the cases tested with real nonuniformity.

Finally, this new technique is applied to infrared data recorded using a 320×240 HgCdTe FPA cooled camera (CEDIP Jade Model) operating in the $8-12\mu\text{m}$ range. The infrared sequence is quantized at 14 bits @ 50fs. As examples, the uncorrected and corrected frames are shown in figures 7, 8. The evolution of \mathbf{P}_k and \mathbf{K}_k are shown in the figure 9. Using the naked eye, it can be seen again a good correction of nonuniformity. However, note that a ghosting artifact is presented in the 1500th frame. Future works will be oriented to develop methodologies to reduce ghosting artifacts, which are generated when a target has been imaged for some time and then it suddenly is out of the field of view of the camera. Our method could not follow such abrupt change in the operation points of the detectors involved in imaging such target.

4 Conclusions

We have developed and tested a new scene-based NUC method based in standard Kalman filter theory. The algorithm has the advantage to use temporal and spatial data embedded in the develop of the Kalman Filter. The param-

eters of the algorithm must to be carefully selected according to the specific application and the kind of infrared camera . The foregoing influences the level of nonuniformity and the level of drift in the nonuniformity parameters. It was experimentally demonstrated as well as by using the performance parameters RMSE and Q that the proposed method is able to reach good performance after processing 500 frames.

References

1. Holst, G.: CCD arrays, cameras and displays. SPIE Optical Engineering Press. Bellingham. (1996).
2. D. A. Scribner, K. A. Sarkady, J. T. Caulfield, M. R. Kruer, G. Katz y C. J. Gridley: Nonuniformity correction for staring IR focal plane arrays using scene-based techniques, SPIE, vol. 1308, pp. 224-233, 1990.
3. D. Scribner, M. Kruer and J. Killiany: Infrared Focal Plane Array Technology, IEEE, vol. 79 (1), pp. 66-85, 1991.
4. D. A. Scribner, K. A. Sarkady, M. R. Kruer, J. T. Caulfield, J. D. Hunt, M. Colbert y M. Descour: Adaptive Retina-Like Preprocessing for Imaging Detector Arrays, IEEE, vol. 3, pp. 1955-1960, 1993.
5. M. Schulz y L. Caldwell: Nonuniformity correction and correctability of infrared focal plane arrays, Infrared Physics and Technology, vol 36, pp. 763-777, 1995.
6. John G. Harris, Yu-Ming Chiang: Non Uniformity Correction Using Constant Statics Constraint: Analog and Digital Implementation, Proc. SPIE 3061 pp. 895-905, 1997.
7. Torres, S., Hayat, M.: Kalman filtering for adaptive nonuniformity correction in Infrared Focal Plane Arrays. The Journal of the Optical Society of America A. **20**. (2003) 470-480.
8. Andrew, H. C.: Forecasting, Structural Time Series Models and the Kalman Filter. Cambridge University Press. (1990).
9. R. E. Kalman: A New Approach to Linear Filtering and Prediction Problems, Transactions of the ASME-Journal of Basic Engineering, 82 (Series D), pp. 35-45. 1960.
10. G. Minkler, J. Minkler, Theory and Application of the Kalman Filtering, Magellan Book Company, 1993.
11. Wang, Z., Bovik, A.: A Universal Image Quality Index. IEEE Signal Processing Letters. **20**. (2002) 1-4.
12. Gonzlez, R., Woods, R.: Digital Image Processing. Addison Wesley. (1993).